

12-29-1986

Scanning Electron Microscopy Study of Particles Generated by Laser Damage of Aluminum Surfaces

L. L. Levenson
University of Colorado

S. D. Traynor
University of Colorado

G. A. Brost
Frank J. Seiler Research Laboratory

F. Ziembo
United States Air Force Academy

Follow this and additional works at: <https://digitalcommons.usu.edu/microscopy>



Part of the [Life Sciences Commons](#)

Recommended Citation

Levenson, L. L.; Traynor, S. D.; Brost, G. A.; and Ziembo, F. (1986) "Scanning Electron Microscopy Study of Particles Generated by Laser Damage of Aluminum Surfaces," *Scanning Microscopy*. Vol. 1 : No. 2 , Article 3.

Available at: <https://digitalcommons.usu.edu/microscopy/vol1/iss2/3>

This Article is brought to you for free and open access by the Western Dairy Center at DigitalCommons@USU. It has been accepted for inclusion in Scanning Microscopy by an authorized administrator of DigitalCommons@USU. For more information, please contact digitalcommons@usu.edu.



SCANNING ELECTRON MICROSCOPY STUDY OF PARTICLES GENERATED BY
LASER DAMAGE OF ALUMINUM SURFACES

L. L. Levenson*, S. D. Traynor, G. A. Brost¹, F. Ziembo²

Department of Physics and Energy Science
University of Colorado
Colorado Springs, CO 80933-7150

¹Frank J. Seiler Research Laboratory,

²United States Air Force,
United States Air Force Academy
Colorado Springs, CO 80840-6528

(Received for publication June 23, 1986, and in revised form December 29, 1986)

Abstract

A high intensity iodine laser (1.315 μm wavelength) was used to study laser-surface damage in vacuum. A 22mm diameter laser beam containing 3.9 J of energy was focused to a 1 mm spot on an aluminum plate mounted in a vacuum chamber. The laser pulse width was 7 μs (FWHM). A copper strip mounted on a quarter circle plate 3.5 cm from the laser spot was used to collect particles ejected from the surface. A scanning electron microscope (SEM) was used to measure the size and spatial distribution of the particles collected on the copper strip. It was found that aluminum droplets were ejected from the crater formed by the laser pulse. The particle sizes ranged from 0.25 to 45 μm in diameter. The peak of the particle size distribution occurred at 1 μm diameter. The maximum spatial distribution of droplets occurred at near 47° from the normal to the target surface. Measurement of the mass lost by the target plate and the volume of aluminum removed from the craters showed that most of the aluminum ejected from the craters remained on the target surface. SEM examination of the surface adjacent to the craters showed that most of the ejected aluminum was liquid splattered around the crater. The particle size and spatial distributions are considered preliminary because droplets smaller than 0.25 μm could not be detected and the copper collector strip was examined in only six areas corresponding to six emission angles.

Key Words: Laser-aluminum surface damage, aluminum droplets, size distribution, spatial distribution.

*Address for correspondence:

L.L. Levenson
Department of Physics and Energy Science
University of Colorado, Colorado Springs,
CO 80933-7150 Phone no.: 303-593-3283

Introduction

The laser has been used for cutting and drilling of various materials for well over a decade. The theory and practice of laser drilling and cutting have been reviewed by several authors [2,6,7,9,10]. In laser metalworking, two important aspects are still not understood in detail. One is the phenomenon of laser-induced reflectivity drop [4,13]. The other is the relationship between the absorbed laser energy and the volume of material removed in the plume of vapor and liquid. The drilling of metals with pulsed lasers occurs via a layer of vapor heated to high pressure on top of a layer of liquid. The high pressure squeezes the liquid out the sides of the hole in the form of droplets [11]. However, the formation of liquid droplets is not always observed. For example, although Ready [8] carried out a theoretical and experimental study of the vaporization of metal by Q-switched lasers, he did not find evidence for droplets although he looked for them. One possible reason why Ready did not find droplets on his focusing lens placed 5 cm away from his target is that his experiments were done in air. However, von Allmen [12] found that a thin transparent sheet in front of a target surface can be used to collect droplets produced by laser drilling. In a theoretical and experimental study, von Allmen [12] showed that the metal drilling efficiency of a Nd-YAG laser is optimal over a fairly narrow range of intensities: roughly from 5 to 50 MW/cm². In this intensity range, von Allmen found that, (1) ejected liquid must come from the bottom of the hole and not from the walls, (2) the liquid jet forms the envelope of a cone, and (3) drilled holes show regular and nearly polished surfaces which suggests a laminar flow of liquid during the ejection process. To date, there have been no detailed studies done on the size and spatial distribution of metal droplets ejected during the formation of craters in metal surfaces by high-power laser pulses. Here, we present preliminary results showing the sizes and spatial distribution of aluminum droplets generated in vacuum by a pulsed iodine laser.

Experimental

The iodine photodissociation laser (IPL) was discovered over twenty years ago and developed in various research laboratories for a variety of applications [1,5]. The IPL has a wave length of 1.31 μm . The IPL used in this study has been described previously [3]. It was operated in the gain-switched mode with multimode pulses of 3.9 J. A 15 cm lens focused the 22 mm beam through a 15 cm vacuum window to a diameter of 1 mm onto a 5 cm square plate of

type 2024 aluminum. Fig. 1 shows a two-dimensional contour of the focused laser beam. A one-dimensional spatial profile of the focused beam is shown in Fig. 2. The temporal pulse profile is given in Fig. 3. The A1 target was mounted inside a vacuum chamber held at a pressure of 20 mTorr. The target was cleaned with acetone before being mounted in the chamber. Measurements with a mechanical profilometer (Sloan Dektak II) showed that the surface roughness was about $\pm 5 \mu\text{m}$. A quarter circle aluminum sheet metal sample holder was mounted next to the target as shown schematically in Fig. 4. Two types of particle collectors were mounted on the sample holder. One was a transmission electron microscope (TEM) grid coated with Formvar and about 20 nm of carbon. The other was a 3 mm wide strip of copper foil. The TEM grid was held to the sample holder with a bit of Scotch tape with the coating facing the focused laser spot. The copper strip was mounted on top of double sided Scotch tape on the inside surface of the sample holder. The experiment was carried out with the laser spot and the particle collector fixed in position. The A1 target was mounted with its surface vertical to the earth's surface. Thus Fig. 4 represents a top view of the target-particle collector configuration. The laser spot was positioned near the top of the target plate. In this way, the target could be rotated 90° after each pulse. (The target and particle collector assembly was removed from the vacuum system after each shot so that the target could be rotated.) After four shots, the target was turned so that four shots could be made on the other side. Eight shots were made on one target. The target was weighed before and after the series of eight shots on a Metler model A163 balance. The accuracy of the balance was 1×10^{-5} gram. The mass lost by the target after eight shots was 320 μg .

A micrograph of a TEM grid placed at 20° from the axis of the laser beam (the angle of incidence of the laser beam was 0°) is shown in Fig. 5. An aluminum droplet impacted on the edge of a grid square. Part of the droplet is bent over the edge of the grid bar. It is apparent that this droplet was hot enough to have a low viscosity when it impacted. A close look at the TEM grid showed that the Formvar coating was destroyed by the laser shots. In Fig. 5 a remnant of the

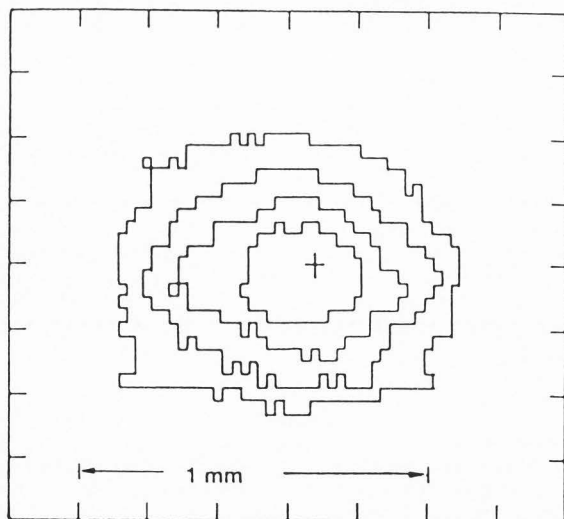


Fig. 1. Two dimensional contour of focused laser beam. Contours are 20, 40, 60 and 80 percent of the peak fluence. The peak fluence point is marked by the cross in the center of the contour pattern.

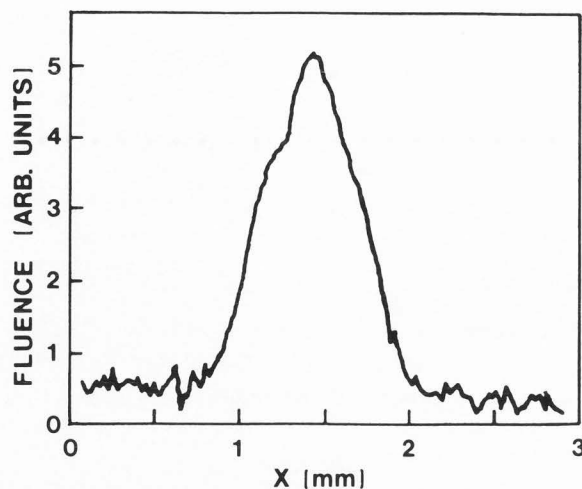


Fig. 2. One-dimensional spatial profile of focused laser beam.

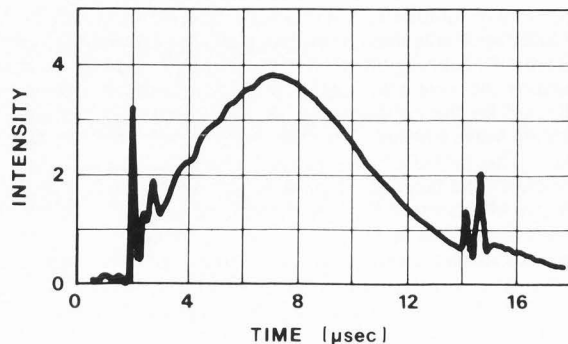


Fig. 3. Temporal pulse profile of laser beam.

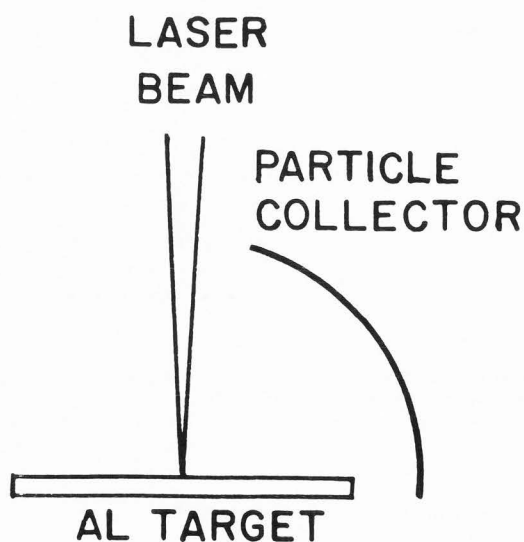


Fig. 4. Schematic sketch of quarter circle particle collector positioned at 3.5 cm from the focal spot of the laser.

SEM Study of Particles Generated by Laser Damage

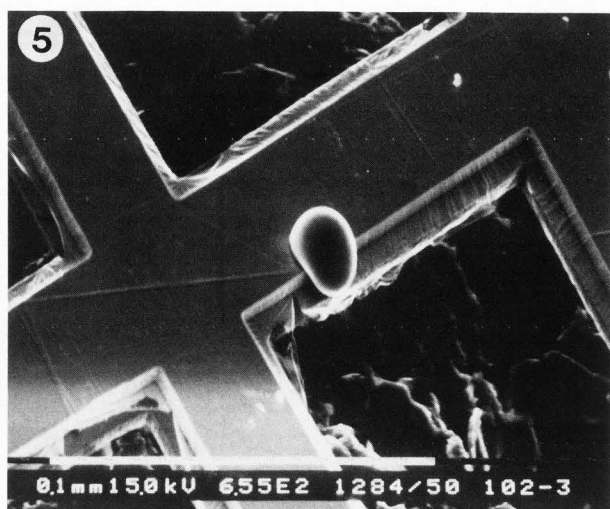
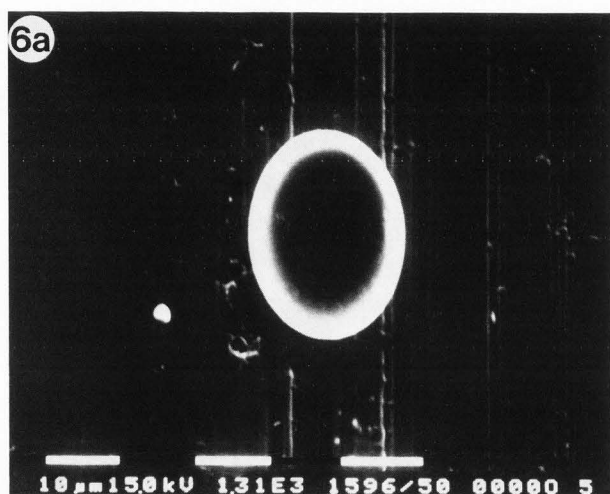


Fig. 5. Aluminum droplet collected on TEM grid. The copper grid was originally coated with about 50 nm of Formvar and 20 nm of carbon. The Formvar and carbon coating was destroyed by the blast of particles from the surface during the laser pulse.



coating can be seen in the corner of the grid opening below the droplet. Thus, in this series of experiments, the TEM grids could not be used in a TEM to determine the size distribution of submicron droplets. The inside radius of the quarter circle particle collector was 3.5 cm. After the series of eight shots on the target, the copper strip was removed from the sample holder and mounted on a steel ruler with pieces of Scotch tape. The steel ruler was attached to an aluminum SEM stub with silver cement and the assembly mounted in the chamber of a Philips model 505 SEM. Areas of 0.1 mm^2 on the copper strip were photographed at six positions which corresponded to different angles from the normal to the target surface. Each area was then divided into four equal areas which were also photographed. Each of the smaller areas were methodically scanned for smooth, egg-shaped particles. These particles were bright against the dark background of the copper strip. Because some contamination particles resembled the aluminum droplets, an EDAX model ECON IV energy dispersive x-ray analyzer was used to confirm the composition of each particle counted as an aluminum droplet. Fig. 6A shows one of the larger droplets along with a small droplet to its lower left. Fig. 6B is an x-ray map of these droplets taken with A1 K level x-rays. The size of each particle was determined by placing its image on the CRT next to the scale bar. The number and size of each A1 droplet was recorded within each 0.1 mm^2 area.

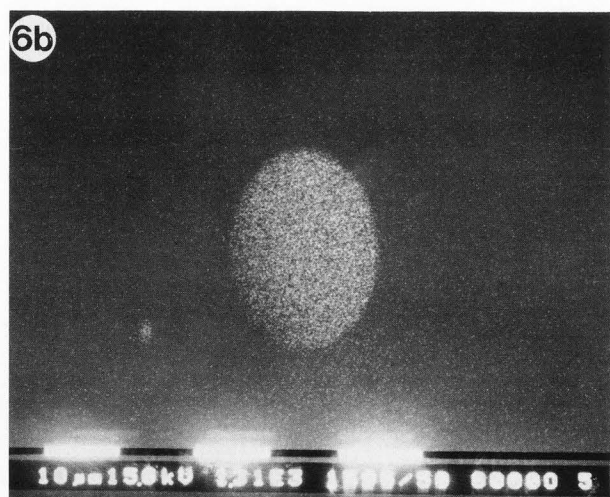


Fig. 6A. Aluminum droplets collected on copper strip at 57° .

Fig. 6B. X-ray map of droplets in Fig. 6A.

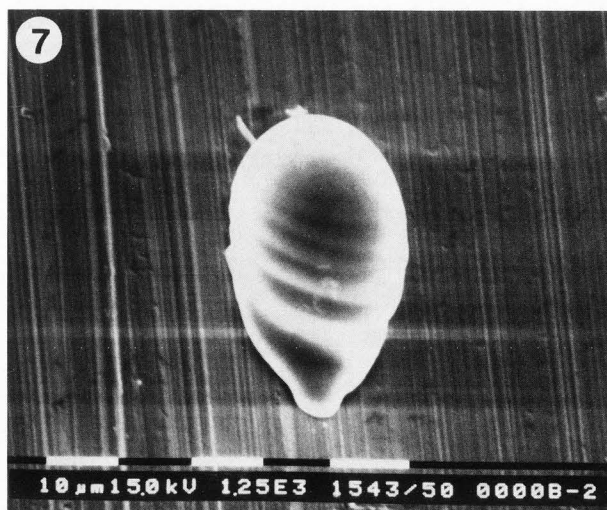


Fig. 7. Aluminum droplet collected on copper strip at 27° .



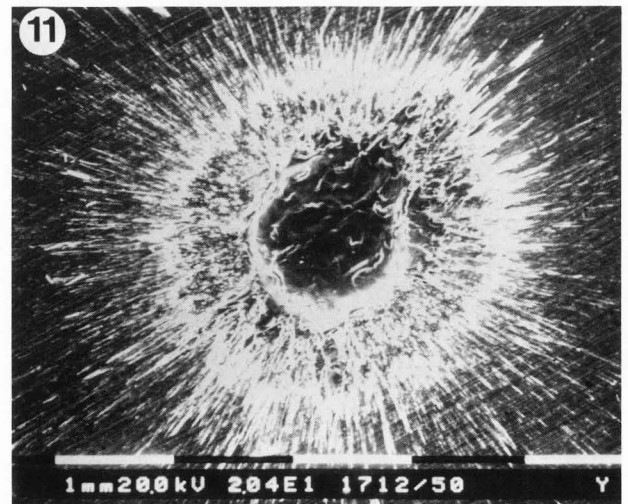
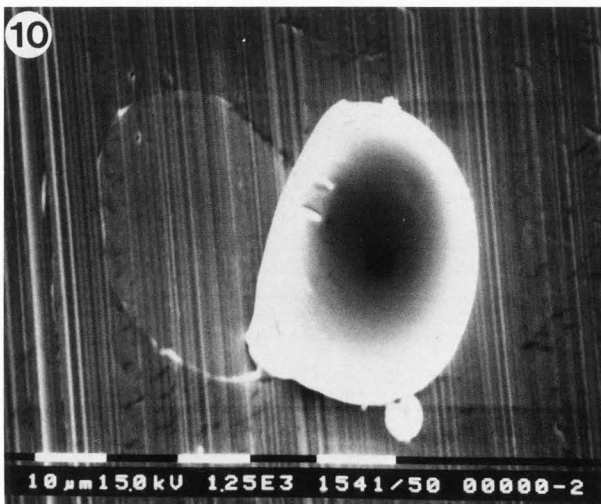
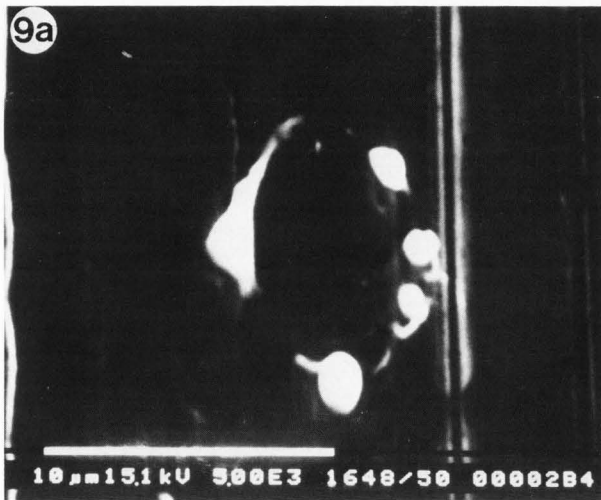
Fig. 8. Aluminum droplet which impacted on copper strip at 71° while still molten.

Fig. 9A. Ring of aluminum droplets left on copper strip at 47° by impact of molten droplet.

Fig. 9B. Impact area of molten droplet at 47° on copper strip.

Fig. 10. Aluminum droplet which has partially bounced after impact at 27° from the target normal.

Fig. 11. Crater and surrounding area on target surface. Smooth bottom and walls indicate liquid flow. Area adjacent to crater is coated with splattered aluminum which was liquid at time of ejection.



SEM Study of Particles Generated by Laser Damage

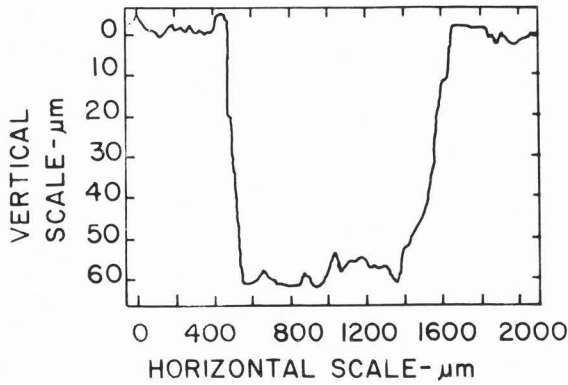


Fig. 12. Profilometer trace of crater. Note difference in vertical and horizontal scales.

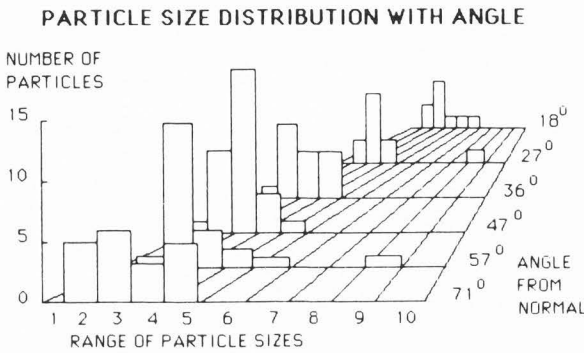
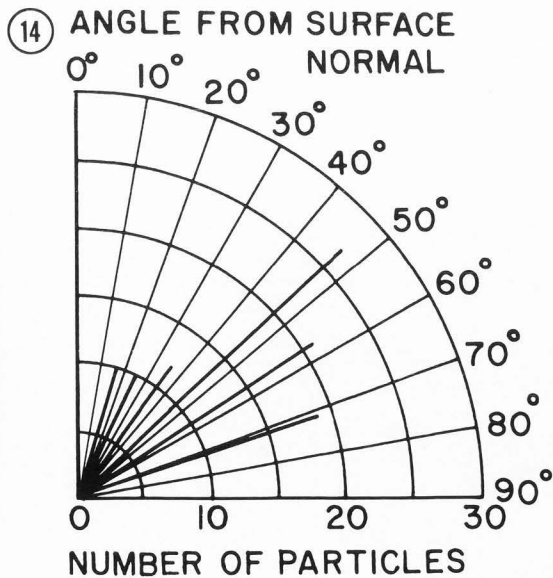


Fig. 13. Three-dimensional plot of droplet size distribution with emission angle. The vertical scale is not constant with emission angle. The numbers in the range of particle sizes correspond to:
 1, $\approx 0.25 \mu\text{m}$; 2, $\approx 0.5 \mu\text{m}$; 3, $\approx 1 \mu\text{m}$; 4, $\approx 2 \mu\text{m}$; 5, $\approx 5 \mu\text{m}$;
 6, $\approx 10 \mu\text{m}$; 7, $\approx 15 \mu\text{m}$; 8, $\approx 20 \mu\text{m}$; 9, $\approx 50 \mu\text{m}$; 10, $\approx 100 \mu\text{m}$.



as seen in Fig. 8. Some droplets impacted and bounced off the ribbon, leaving behind a ring of droplets as seen in Figs. 9A and 9B. These ring impressions were the only ones observed in the six selected 0.1 mm^2 areas. A couple of droplets were recorded to have partially bounced but remained stuck to the surface as in Fig. 10. The ring of aluminum outlining the particle's shape upon impact is clearly seen. From these observations, it is apparent that while most droplets were solid upon impact at a distance of 3.5 cm from the laser focal point, some were still molten or partially molten. The craters generated by the laser pulses showed smooth, but rippled bottoms and walls as shown in Fig. 11. A ring of splattered fluid aluminum radiated out from the crater during the pulse. A profilometer trace of a crater is shown in Fig. 12. The craters were about $60 \mu\text{m}$ deep and about $1200 \mu\text{m}$ wide at the top. The mass of aluminum represented by the volume of the eight craters is about $1000 \mu\text{g}$. Since only $320 \mu\text{g}$ was lost by the target plate, one must conclude that much of the aluminum ejected from the craters remains on the target surface as splattered liquid. The sizes of the droplets were put into ten size categories. These size categories are shown in Table 1, which shows the size distribution for each of the six 0.1 mm^2 areas at the selected angles.

TABLE 1
 NUMBER OF DROPLETS AS FUNCTION OF SIZE AND ANGLE

ANGLE SIZE μm	18° No.	27° No.	36° No.	47° No.	57° No.	71° No.
≈ 0.25	0	0	1	1	0	0
≈ 0.5	2	2	5	7	1	5
≈ 1	5	5	3	14	12	6
≈ 2	1	2	3	4	4	3
≈ 5	1	0	0	1	2	5
≈ 10	1	0	0	0	1	0
≈ 15	0	0	0	0	0	0
≈ 20	0	0	0	0	0	0
≈ 50	0	1	0	0	1	0
≈ 100	0	0	0	0	0	0
Total No.	10	10	12	27	21	19

The size distribution in Table 1 is plotted in Fig. 13. It is apparent that the distribution peaks for droplets that are about $1 \mu\text{m}$ in diameter. Unfortunately, the size distribution of droplets smaller than $0.25 \mu\text{m}$ could not be measured because of the destruction of the TEM grid coatings by the material ejected from the craters. The total number of droplets found in each area as a function of angle is shown in a polar plot in Fig. 14. From Table 1 and from Fig. 14 it is apparent that the largest number of droplets is projected in direction close to 47° . The two large droplets found at 27° and 57° , if counted in the mass distribution, would cause two peaks in the mass distribution in those directions. However, the statistics of this distribution are too weak to permit any conclusions to be made for the mass distribution.

Fig. 14. Polar plot of the total number of droplets found by SEM examination of each of 0.1 mm^2 areas at various angles from the normal to the target surface.

Conclusions

Results obtained with a pulsed iodine laser focused to 1 mm spot size on the surface of type 2024 aluminum indicate that aluminum droplets are ejected in all directions with a peak of the number density near 47° from the surface normal. In this study, the angle of incidence of the laser beam was 0° and the energy of the beam was 3.9J. The average mass lost by the target per pulse was 40 μg although the mass ejected from a crater averaged 125 μg . From micrographs of the area around each crater, it appears that most of the mass ejected from the craters is splattered liquid which is deposited on the surface around the crater. A SEM survey of a copper strip mounted in a quarter circle at 3.5 cm from the laser spot showed that aluminum droplets were ejected in all directions from the craters, with a peak of the number distribution near 47° . The size distribution of the droplets showed a peak at about 1 μm diameter. SEM observation showed that most of the aluminum droplets were solid when they hit the copper collector, but a significant number were molten or partially molten. These observations are in accord with the model of liquid ejection developed by von Allmen [12].

Acknowledgements

We want to thank Mr. Leonard Gilbert for making the quarter circle collector holder in the machine shop of the Department of Physics and Energy Science at the University of Colorado-Colorado Springs. The support of Captain C.L. Bohn, Department of Physics, U.S.A.F.A. and Professor C. Araujo, Microelectronics Research Laboratory, Department of Electrical Engineering, U.C.C.S. is gratefully acknowledged.

References

1. Bannister JJ, King TA. (1983). The Atomic Iodine Photodissociation Laser, Laser Focus/Electro-Optics, August 88-96.
2. Bertolotti M. (1983). Physical Processes in Laser-Materials Interactions, Plenum Press, New York. pp. 109-110, 159-161, 302-307, 311, 469-474.
3. Bohn CL, Stephen MD, Eng F, Souders JC, Brost GA, Deaton TF, Duvall BW, Tinsley JT (1985). Mechanical Coupling of Iodine Laser Pulse Incident Obliquely on Aluminum, SPIE 540, 290-294.
4. Bonch-Bruevich AM, Imas YaA, Romanov GS, Libenson MN, Mal'tsev LN. (1968). Effect of a Laser Pulse on the Reflecting Power of a Metal, Sov. Phys.-Tech. Phys. 13, 640-643.
5. Brederlow G, Fill E, Witte KJ. (1983). The High Power Iodine Laser, Springer-Verlag, New York. pp.1-3.
6. Duley WW. (1976). CO₂ Lasers: Effects and Applications, Academic Press, New York. pp. 205-210, 248-251.
7. Duley WW. (1983). Laser Processing and Analysis of Materials, Academic Press, New York. pp. 108-109, 134-137.
8. Ready JF. (1965). Effects due to the Absorption of Laser Radiation, J. Appl. Phys. 10, 462-468.
9. Ready JF. (1971). Effects of High Power Laser Radiation, Academic Press, New York. pp. 378-379, 386-389.
10. Ready JF. (1978). Industrial Applications of Lasers, Academic Press, New York.

11. Uglov AA, Kokora AN. (1977). Thermophysical and Hydrodynamic Effects in Laser-Beam Processing of Materials (review), Sov. J. Quantum Electronics 7, 671-678.
12. von Allmen M. (1976). Laser Drilling Velocity in Metals, J. Appl. Phys. 47, 5460-5463.
13. von Allmen M, Blaser P, Affolter K, Stürmer E. (1978). Absorption Phenomena in Metal Drilling with Nd-lasers, IEEE J. Quantum Electron. QE-14, 85-88.

Discussion with Reviewers

H.Seiler: Do you have any information on the temperature reached in the impact point of the laser on the surface?

Authors: We have made no attempt to measure the temperature reached at the impact point. However, it is evident that the aluminum vapor pressure reached at the impact point was sufficient to force liquid aluminum out of the crater.

J.A. Brown: What practical application to laser welding, etc. can be made with the technical data found?

Authors: Our data is too limited to be applied directly to laser welding or drilling. However, it does support von Allmen's theory and experimental data concerning laser drilling (Refs. 12, 13).